Key to the mandibles of small mammals of eastern Canada

A. General key to small mammals

1a. Wide diastema between the incisor and molars (Figure 2A) 2
1b. No diastema between the incisor and molars (Figure 2B) 3

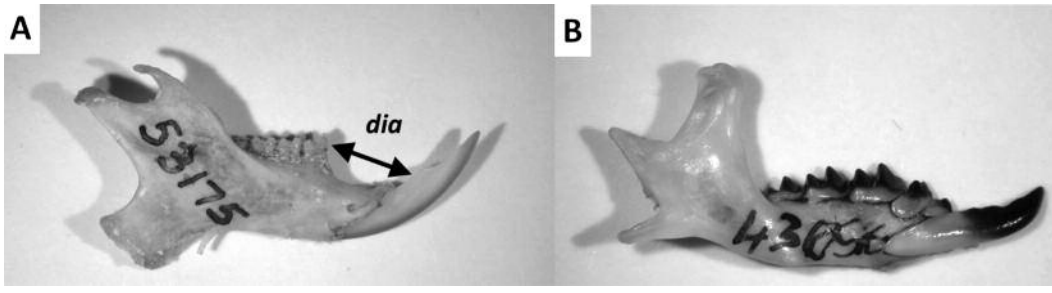

FIGURE 2. (*labial view*) Dentary bone of rodents with a large diastema (*dia*) (*Glaucomys volans*) (A), and soricomorphs (*Blarina brevicauda*) (B).

2a. Two premolars and three molars; coronoid process and condylar process not differentiated or coronoid process minute (Figure 3A) . . . . . Lagomorpha (section B) 5
2b. One premolar or none and three molars; coronoid process clearly differentiated from the condylar process (Figure 3B) . . . . . Rodentia (section C) 7

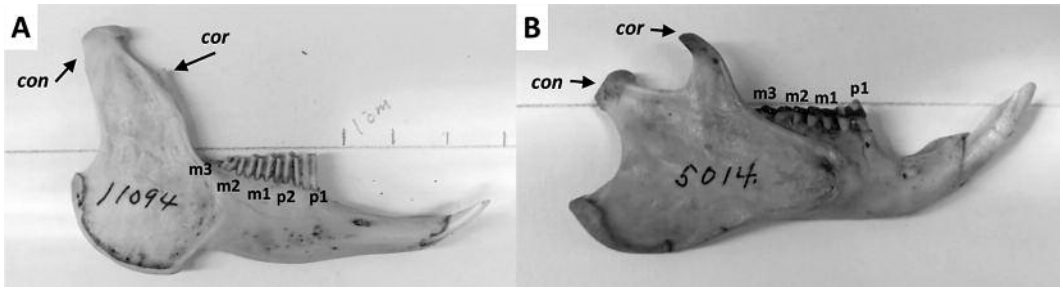

FIGURE 3. (*labial view*) Coronoid (*cor*) and condylar (*con*) processes of lagomorphs (*Lepus arcticus*) (A) and rodents (*Marmota monax*) (B).

3a. Canines and premolars similar in size; well-developed angular process that is often the most posterior part of the dentary bone (Figure 4A) . . . . . .Soricomorpha (section D) 31
3b. Canines two to three times the size of the adjacent premolar; small but robust angular process . . . . . (Figure 4B) 4

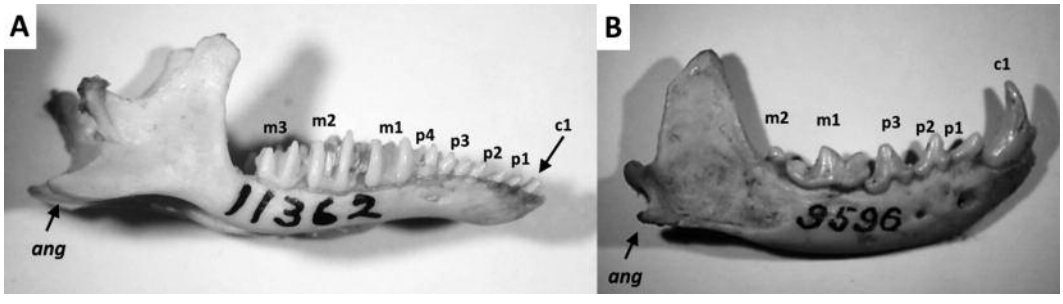

FIGURE 4. (*labial view*) Size of the angular process as well as the size of the canine compared to the adjacent premolar in soricomorphs (*Parascalops breweri*) (A) and carnivores (*Neovison vison*) (B).

4a. The most posterior molar often much smaller than the most anterior molar; lower edge of ramus without a bump under the canine; height of the coronoid process much higher than the height of the condylar process (Figure 5A) . . . . . Carnivora (section E) 42
4b. Three W-shaped molars of similar size; lower edge of ramus with a bump under the canine; height of the coronoid process similar in size to or slightly higher than the height of the condylar process (Figure 5B) . . . . . Chiroptera (section F) 50

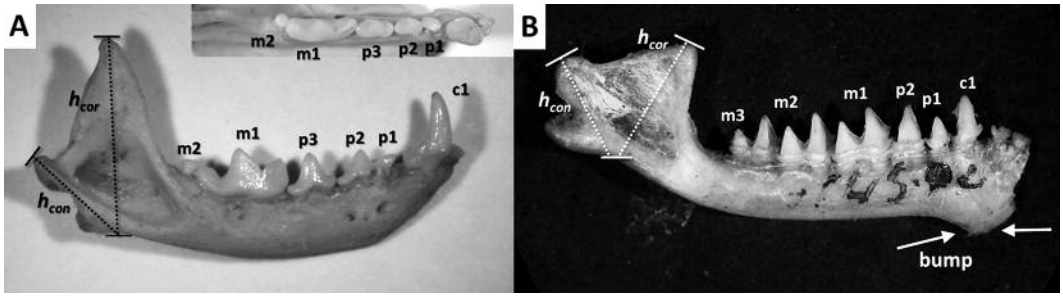

FIGURE 5. (*labial view*) Dentary bones of carnivores (*Mustela erminea*) (A) and chiropterans (*Perimyotis subflavus*) (B) with the height of the condylar process (h_{con}), height of the coronoid process (h_{cor}), and the conspicuous mandibular bump of chiropterans.

B. Lagomorpha (Leporidae)

5a. Height of coronoid process >40 mm; length of mandibular tooth row >16 mm (Figure 6A) . . . . . *Lepus arcticus*, *L. townsendii*, *L. europaeus*
5b. Height of coronoid process <40 mm; length of mandibular tooth row <16 mm (Figure 6B) 6

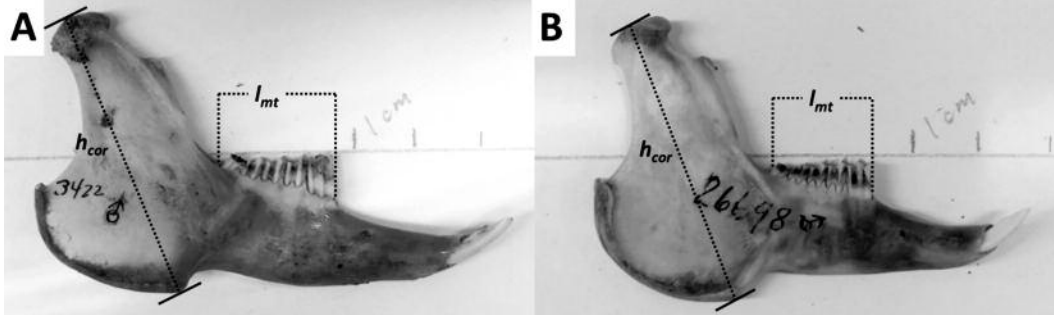

FIGURE 6. (*labial view*) Height of the coronoid process (h_{cor}) and the length of the mandibular toothrow (l_{mt}) measured on lagomorphs (*Lepus townsendii* (A) and *Lepus americanus* (B)).

6a. Mental foramen easily visible from the occlusal view (Figure 7A) . . . . . *Sylvilagus floridanus*
6b. Mental foramen barely visible from the occlusal view (Figure 7B) . . . . . *Lepus americanus*

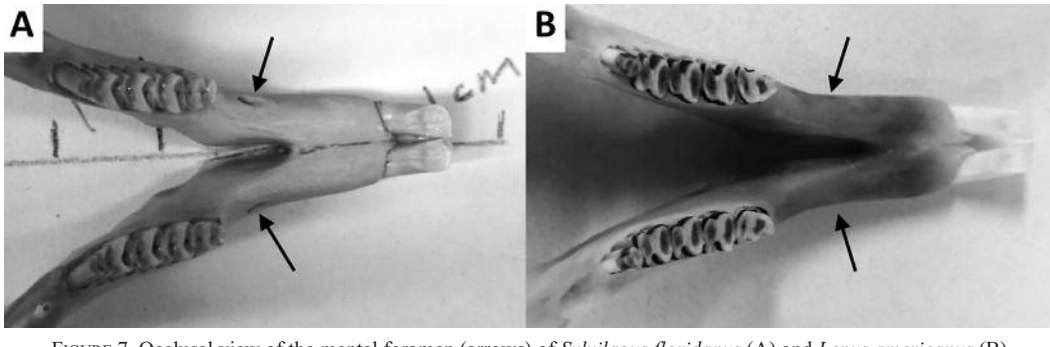

FIGURE 7. Occlusal view of the mental foramen (arrows) of *Sylvilagus floridanus* (A) and *Lepus americanus* (B).

C. Rodentia (Cricetidae, Dipodidae, Erethizontidae, Muridae, and Sciuridae)

7a. Lower edge of horizontal ramus with sharp angle under p1 (Figure 8A); angular process clearly smaller than the coronoid process; cheek teeth with closed circular patterns of enamel (Figure 8B) . . . . . *Erethizon dorsatum*

7b. Lower edge of horizontal ramus smooth; the coronoid process and the angular process are similar in size or the angular process is larger than the coronoid process; cheek teeth with triangular patterns of enamel or without clearly defined patterns 8

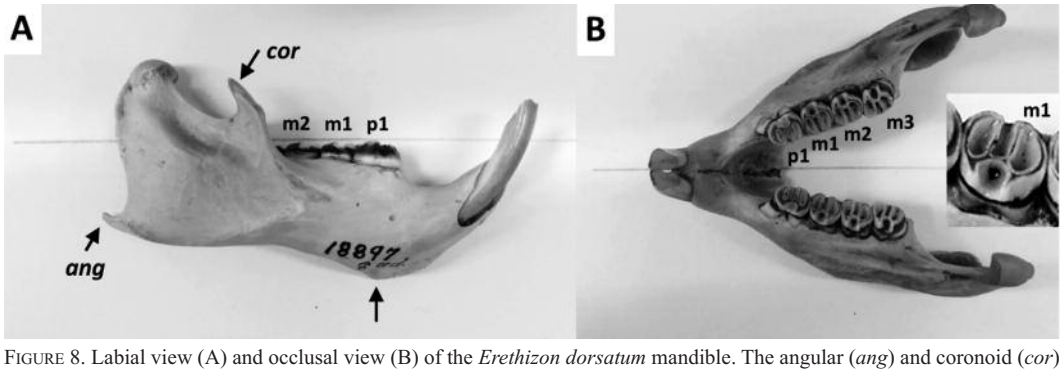

FIGURE 8. Labial view (A) and occlusal view (B) of the *Erethizon dorsatum* mandible. The angular (*ang*) and coronoid (*cor*) processes are indicated by the arrows.

8a. Angular process clearly the most exterior part of the mandible (Figure 9A); angular process about twice as wide labially as the condylar process (Figure 9A); anterior edge of the coronoid process that connects with the angular process creates a bump pointing outwards at the level of p1-m1 in the occlusal view (Figure 9B); . . . . . *Marmota monax*

8b. The condylar process or the coronoid process is the most exterior part of the mandible (occlusal view); no bumps created by the edge of the coronoid and angular processes next to p1-m1; angular process about the same labial thickness or less than the condylar process 9

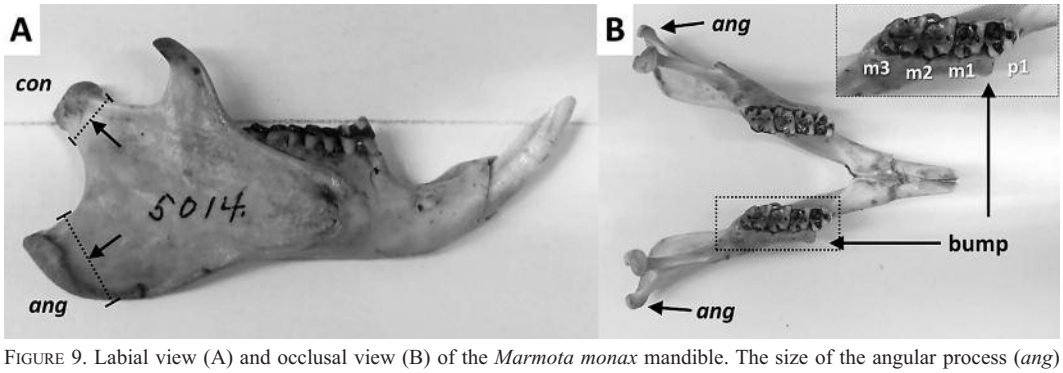

FIGURE 9. Labial view (A) and occlusal view (B) of the *Marmota monax* mandible. The size of the angular process (*ang*) compared to the condylar process (*con*) is shown in A and the bump near p1 and m1 is shown in B.

9a. Tip of the angular process clearly higher than the teeth (Figure 10A) . . . . . *Ondatra zibethicus*

9b. Tip of the angular process below or even with the teeth (Figure 10B) 10

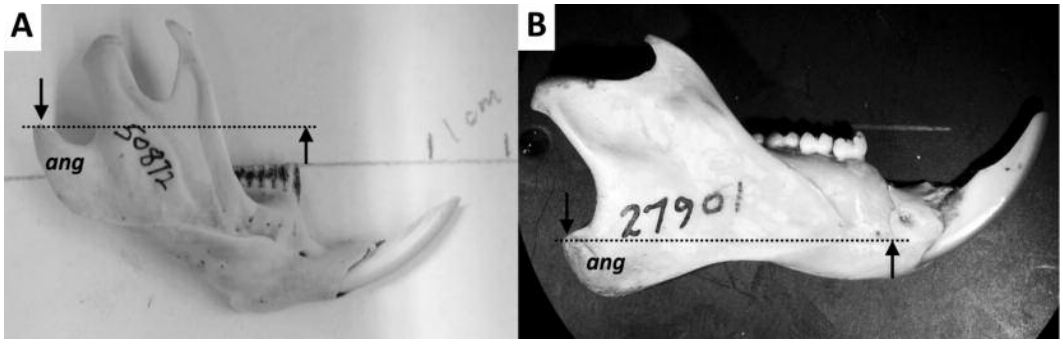

FIGURE 10. (*labial view*) Height of the angular process (arrows) of *Ondatra zibethicus* (A) and sciurids (*Sciurus niger*) (B).

10a. One premolar (Figure 11A); angular process extends slightly behind the coronoid process (Figure 11C) 11
10b. No premolar (Figure 11B); angular process extends well behind the coronoid process (Figure 11D) 18

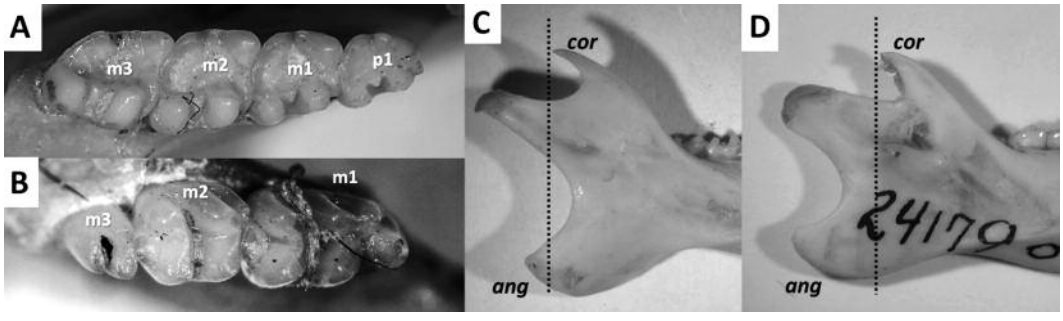

FIGURE 11. (*A and B. occlusal view*; *C and D. labial view*) Dental formula of squirrels (*Glaucomys sabrinus*) (A) and of Cricetidae, Dipodidae, and Muridae (*Mus musculus*) (B) and the angular (*ang*) and coronoid (*cor*) processes of squirrels (*G. sabrinus*) (C) and of other rodents (*Rattus norvegicus*) (D).

11a. Coronoid process long; size of the notch between the coronoid and condylar processes similar in size to the notch between the condylar and angular processes (Figures 12A and 12B) 12
11b. Coronoid process relatively short; size of the notch between the coronoid and condylar processes clearly smaller than the notch between the condylar and angular processes (Figures 12C and 12D) . . 14

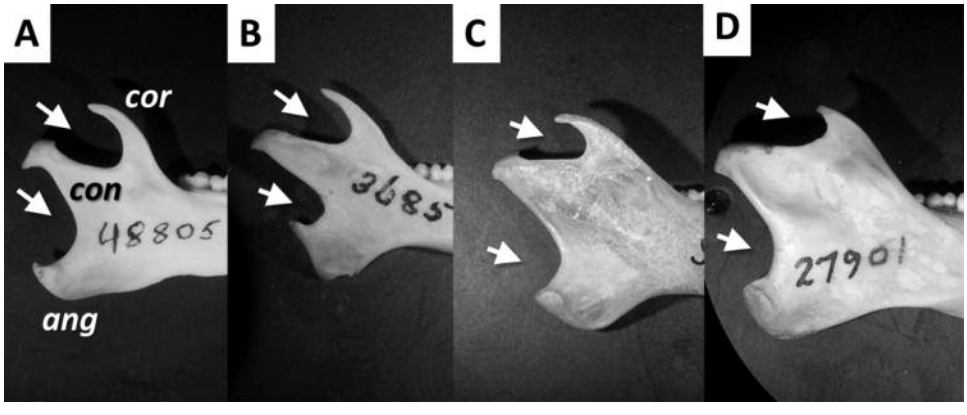

FIGURE 12. (*labial view*) Notches (arrows) created by the coronoid (*cor*), condylar (*con*), and angular (*ang*) processes of *Poliocitellus franklinii* (A), *Tamias minimus* (B), *Tamiasciurus hudsonicus* (C), and *Sciurus niger* (D).

12a. T-shaped condylar process; angular and condylar processes equally posterior (Figure 12A) . . . . . *Poliocitellus franklinii*
12b. A-shaped condylar process; condylar process clearly the most posterior component of the ramus (Figure 12B) 13

13a. Length of the mandibular tooth row <5.5 mm . . . . . *Tamias minimus*
13b. Length of the mandibular toothrow >5.5 mm . . . . . *Tamias striatus*

14a. Height of the coronoid process >17 mm; length of the mandibular tooth row >35 mm 15
14b. Height of the coronoid process <17 mm; length of the mandibular tooth row <35 mm 16

15a. Coronoid process short; notch created by the coronoid process and the condylar process appears wide open; lower tip of the angular process appears squared (Figure 13A) . . . . . *Sciurus niger*
15b. Coronoid process longer; coronoid notch narrow; lower tip of the angular process appears rounded (Figure 13B) . . . . . *Sciurus carolinensis*

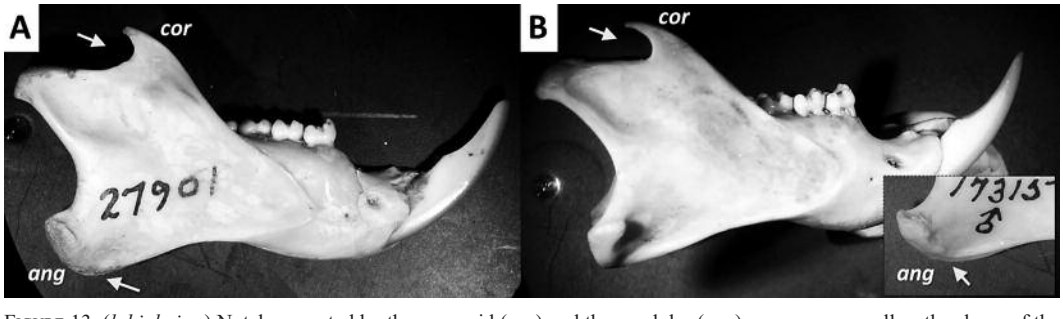

FIGURE 13. (*labial view*) Notches created by the coronoid (*cor*) and the condylar (*con*) processes as well as the shape of the lower part of the angular process of *Sciurus niger* (A) and *S. carolinensis* (B).

16a. Uppermost edge of the condylar process relatively flat (Figure 14A) . . . . . *Tamiasciurus hudsonicus*
16b. Uppermost edge of the condylar process concave (Figure 14B) 17

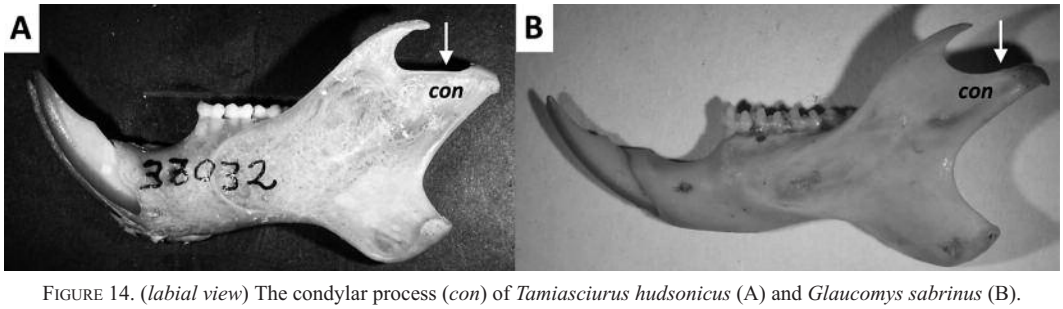

FIGURE 14. (*labial view*) The condylar process (*con*) of *Tamiasciurus hudsonicus* (A) and *Glaucomys sabrinus* (B).

17a. Posterior tip of the angular process above the notch on the lower edge of the horizontal ramus (Figure 15A) . . . . . *Glaucomys volans*
17b. Posterior tip of the angular process below or at the same level as the notch on the lower edge of the horizontal ramus (Figure 15B) . . . . . *Glaucomys sabrinus*

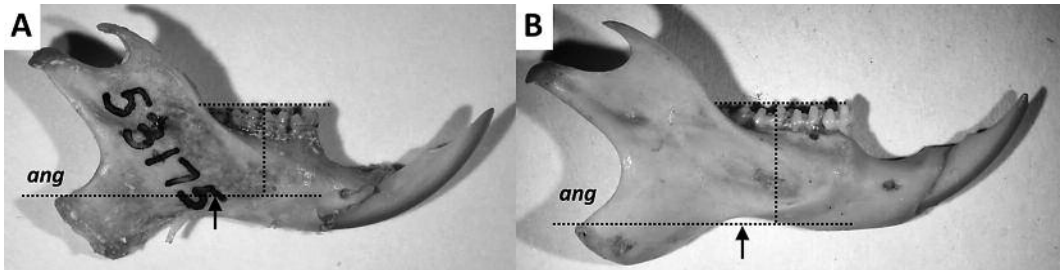

FIGURE 15. (*labial view*) Relative position of the upper part of the angular process (*ang*) in relation to the notch created by the lower edge of the ramus of *Glaucomys volans* (A) and *G. sabrinus* (B).

18a. Molars without re-entrant angles or closed triangles (Figure 16A) 19
18b. Molars with well-defined lingual and labial re-entrant angles (Figure 16B), often with closed triangles of enamel (Figure 16C) 23

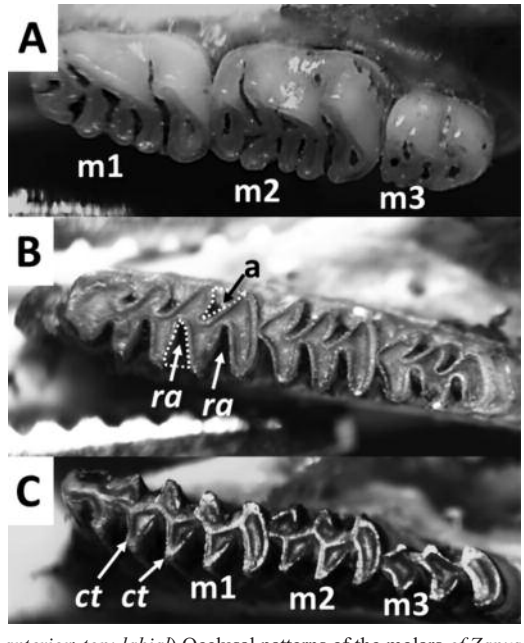

FIGURE 16. (*occlusal view*; *left: anterior*; *top: labial*) Occlusal patterns of the molars *of Zapus hudsonius* (A), *Myodes gapperi* (B), and *Microtus pennsylvanicus* (C). The labels refer to re-entrant angles (*ra*) and closed triangles of enamel (*ct*).

19a. Condylar process clearly the most posterior part of the dentary bone; coronoid process small, at about the same height as the condylar process (Figure 17A) . . . . . *Peromyscus leucopus* or *P. maniculatus*
19b. Condylar process slightly posterior to the angular process or about equally posterior; coronoid process relatively long and higher than the condylar process (Figure 17B) 20

20a. Molars with complex patterns of enamel loops (Figure 18A) 21
20b. Molars with simple patterns of enamel loops (Figures 18B and 18C) 22

21a. Anteromedian fold present on m1; anteroconid of m1 clearly separated from the protoconid by the preprotoconid and premetaconid folds (Figure 19A) . . . . . *Zapus hudsonius*
21b. Anteromedian fold absent on m1; anteroconid of m1 not separated or slightly separated from the protoconid by the premetaconid fold (Figure 19B) . . . . . *Napaeozapus insignis*

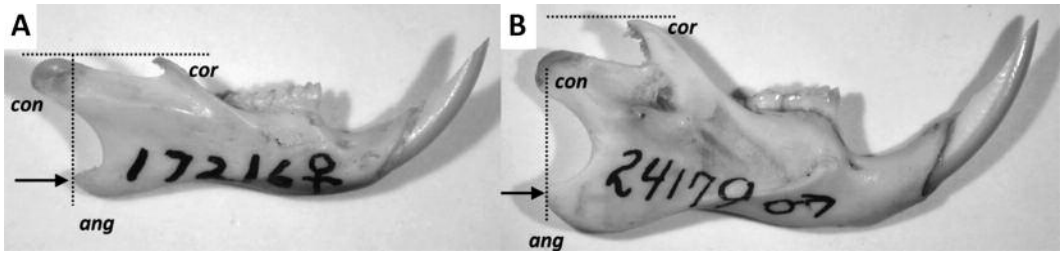

FIGURE 17. (*labial view*) Relative shape, size, and position of the coronoid (*cor*), condylar (*con*), and angular (*ang*) processes of *Peromyscus leucopus* (A) and *Rattus norvegicus* (B).

22a. Molars with simple patterns of enamel (Figure 20A) . . . . . *Mus musculus*
22b. Molars with two rows of cusps without patterns of enamel (Figure 20B) . . . . . *Rattus norvegicus*

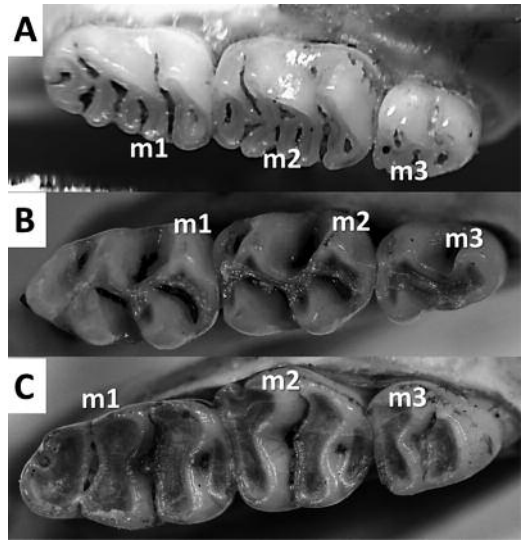

FIGURE 18. (*occlusal view*; *left: anterior*; *top: labial*) Occlusal patterns of the molars of *Zapus hudsonius* (A), *Mus musculus* (B), and *Rattus norvegicus* (C).

23a. Re-entrant angles of molars much deeper on lingual side than on labial side (Figures 21A, 21B, and 21C) 24
23b. Re-entrant angles of molars equal in size on both lingual and labial side (Figures 21D, 21E, 21F, 21G, 21H, and 21I) 26

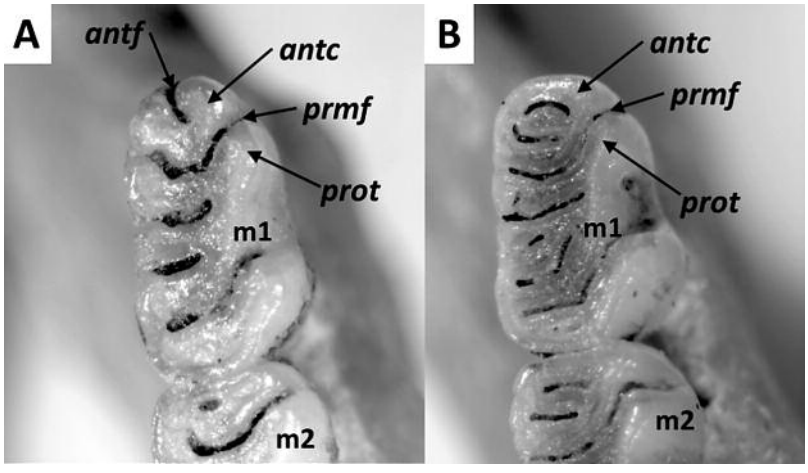

FIGURE 19. (*occlusal view*; *left: lingual*; *top: anterior*) Occlusal pattern of m1 in *Zapus hudsonius* (A) and *Napaeozapus insignis* (B). The labels refer to the anteromedian fold (*antf*), the anteroconid (*antc*), the premetaconid fold (*prmf*), and the protoconid (*prot*).

24a. Brachydont teeth (molars closed-rooted) (Figures 22A, 22B, 22C, 23A, and 23B); several small closed triangles on the labial side of molars (Figure 21A) . . . . . *Phenacomys ungava*
24b. Hypsodont teeth (molars open-rooted) (Figures 22D and 23C); one closed triangle or none on the labial side of each molar (Figures 21B and 21C) 25

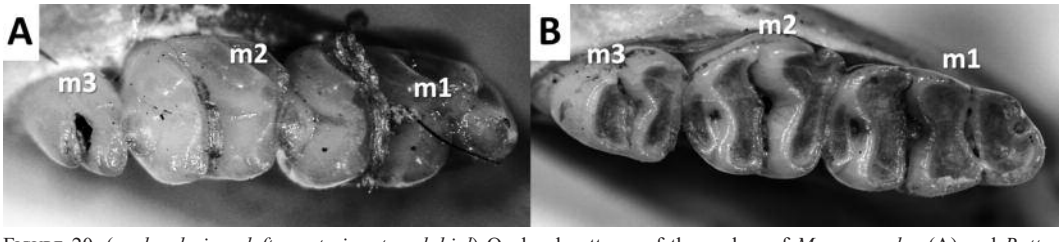

FIGURE 20. (*occlusal view*; *left: posterior*; *top: labial*) Occlusal patterns of the molars of *Mus musculus* (A) and *Rattus norvegicus* (B).

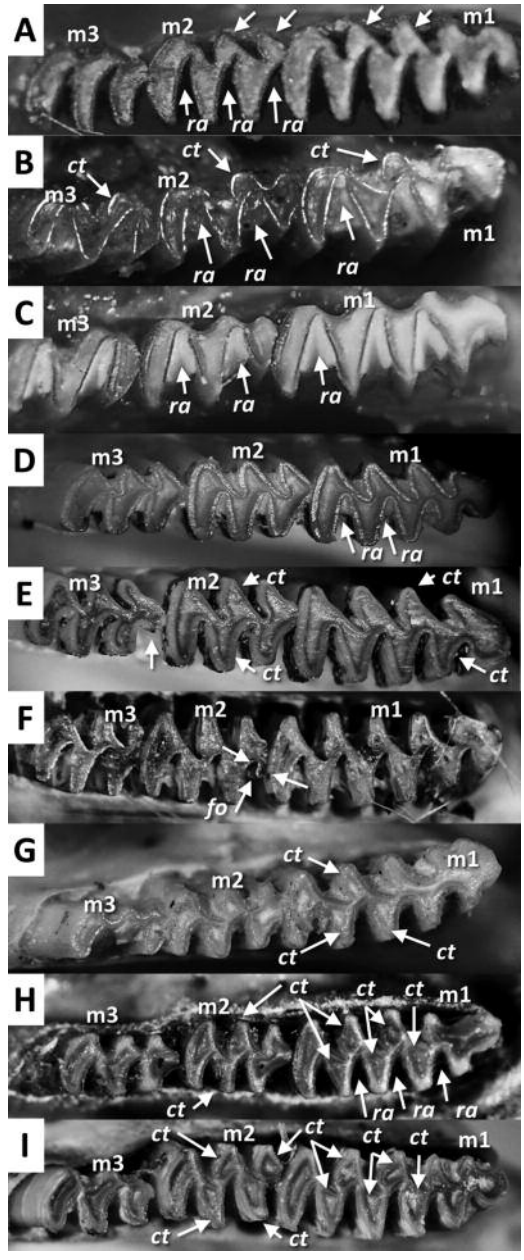

FIGURE 21. (*occlusal view*; *left: posterior*; *top: labial*) Occlusal patterns with re-entrant angles (*ra*), closed triangles (*ct*) and folds of enamel (*fo*) of the molars of *Phenacomys ungava* (A), *Synaptomys cooperi* (B), *Synaptomys borealis* (C), *Myodes gapperi* (D), *Myodes glareolus* (E), *Dicrostonyx hudsonius* (F), *Microtus pinetorum* (G), *Microtus chrotorrhinus* (H), and *Microtus pennsylvanicus* (I).

25a. A single closed triangle on the labial side of each molar (Figure 21B) . . . . . *Synaptomys cooperi*
25b. No closed triangle on the labial side of molars (Figure 21C) . . . . . *Synaptomys borealis*

26a. Brachydont teeth (molars closed-rooted) (Figures 22A, 22B, 22C, 23A, and 23B); occlusal triangles of molars rounded and "enclosed" by the enamel borders (Figures 21D and 21E) 27
26b. Hypsodont teeth (molars open-rooted) (Figures 22D and 23C); occlusal closed triangles with sharp tips (Figures 21F, 21G, 21H, and 21I) 28

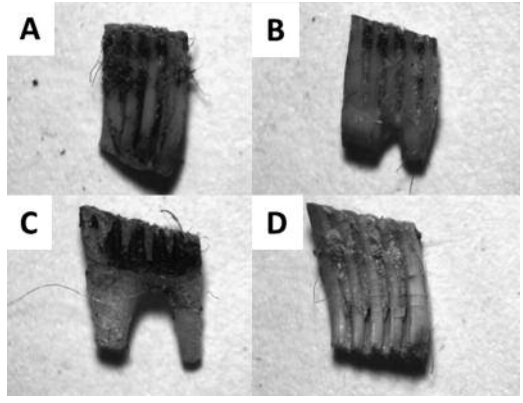

FIGURE 22. (*labial view*) Brachydont teeth in their early stages (*Myodes gapperi*) (A), middle stages (*M. gapperi*) (B), and late stages (*Phenacomys ungava*) (C) and hypsodont teeth (*Microtus pennsylvanicus*) (D).

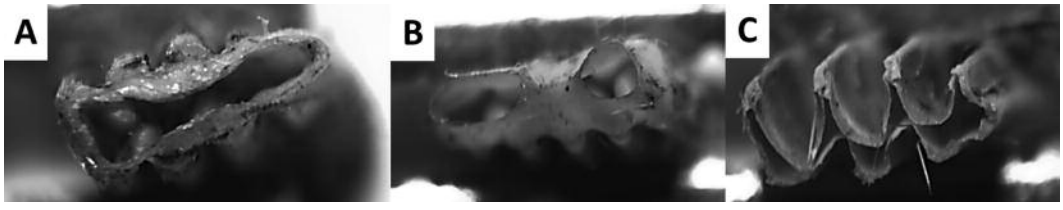

FIGURE 23. (*bottom view*) Base of brachydont teeth in their early stages (*Myodes gapperi*) (A) and middle stages (*M. gapperi*) (B) and of hypsodont teeth (*Microtus pennsylvanicus*) (C).

27a. Occlusal triangular shapes of enamel of m1 and m2 often connected by wide bridges; shape of the anterior triangle of m3 is typically similar to the posterior triangles (Figure 21D) . . . . . *Myodes gapperi*
27b. Occlusal triangles on m1 and m2 often connected by narrow bridges; shape of the anterior triangle of m3 often different from the other triangles (Figure 21E) . . . . . *Myodes glareolus*

28a. Presence of a small fold of enamel on the anterior and lingual side of m2 (Figure 21F) . . . . . *Dicrostonyx hudsonius*
28b. Absence of a small fold of enamel on the anterior and lingual side of m2 (Figures 21G, 21H, and 21I) 29

29a. Three closed triangles on m1 (Figure 21G) . . . . . *Microtus pinetorum*
29b. Five closed triangles on m1 (Figures 21H and 21I) 30

30a. Two closed triangles on m2 (Figure 21H) . . . . . *Microtus chrotorrhinus*
30b. Four closed triangles on m2 (Figure 21I) . . . . . *Microtus pennsylvanicus*

D. Soricomorpha (Soricidae and Talpidae)
31a. Teeth all white; incisors without a posterior cusp; alveolus of incisors does not extend under premolars or molars (Figure 25A) 32
31b. Tip of teeth often with red and/or brown pigments; incisors with a posterior cusp; alveolus of incisors extends beneath the first premolar or posteriorly (Figures 24 and 25B) 34

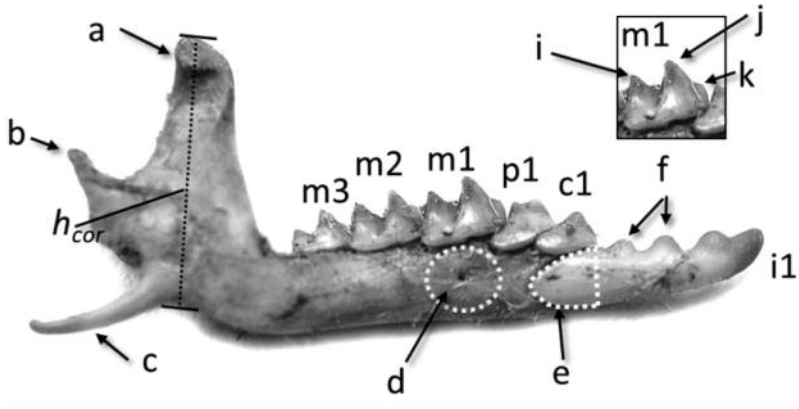

FIGURE 24. (*labial view*) Schematic overview of the shrew dentary bone: coronoid process (a), condylar process (b), angular process (c), mental foramen (d), alveolus of the incisor (e), posterior cusp of the incisor (f), hypoconid (i), protoconid (j), paraconid (k), and height of the coronoid process (h_{cor}).

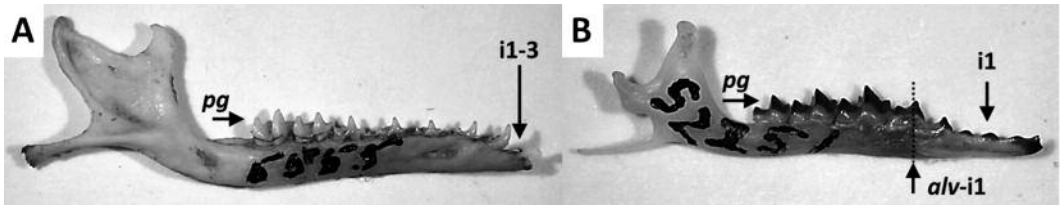

FIGURE 25. (*labial view*) Dentary bones of moles (A) and shrews (B). The labels are as follows: pigmentation (*pg*) and alveolus of the incisor (*alv*-i1). The depth of the incisor alveolus in relation to p1 is shown in B (arrow).

32a. Two incisors, no canine, and three premolars; presence of a short diastema between the second incisor and the first premolar (Figure 26A) . . . . . *Scalopus aquaticus*
32b. Three incisors, one canine, and four premolars; presence of several short diastemata between the premolars (Figure 26B) or complete absence of diastemata (Figure 26C) 33

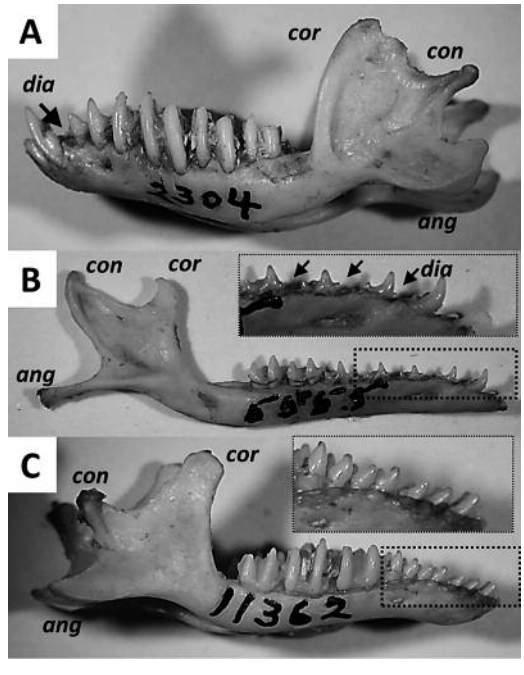

FIGURE 26. (*labial view*) Dentary bones of the three moles (Talpidae) present in eastern Canada: *Scalopus aquaticus* (A), *Condylura cristata* (B), and *Parascalops breweri* (C). The labels refer to the coronoid process (*cor*), condylar process (*con*), angular process *(ang*), and diastema (*dia*).

33a. Canine and the first three premolars separated by short diastemata; angular process long and slender; condylar process about the same height as the coronoid process or higher; coronoid process clearly smaller than the condylar process (Figure 26B) . . . . . *Condylura cristata*
33b. Canine and first three premolars not separated by diastemata; coronoid process higher than the condylar process; coronoid larger than the condylar process (Figure 26C) . . . . . *Parascalops breweri*

34a. Alveolus of incisor extends slightly or substantially beneath m1; alveolus extends at the level of the m1 paraconid or posteriorly (Figure 27A) 35
34b. Alveolus of incisor does not extend beneath the m1 paraconid (Figure 27B) 36

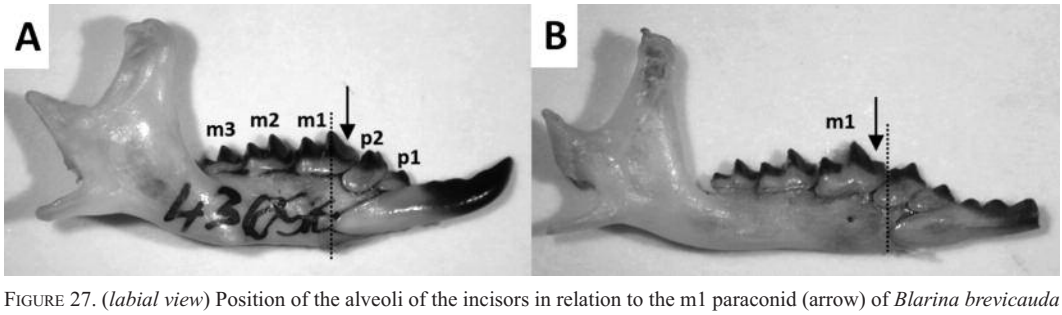

FIGURE 27. (*labial view*) Position of the alveoli of the incisors in relation to the m1 paraconid (arrow) of *Blarina brevicauda* (A) and *Sorex hoyi* (B).

35b. Three small cusps on the occlusal surface of the incisor; angular process long and very slender (Figure 28A) . . . . . *Sorex hoyi*
35a. One or two small cusps on the occlusal surface of the incisor; angular process relatively short and robust (Figure 28B) . . . . . *Blarina brevicauda*

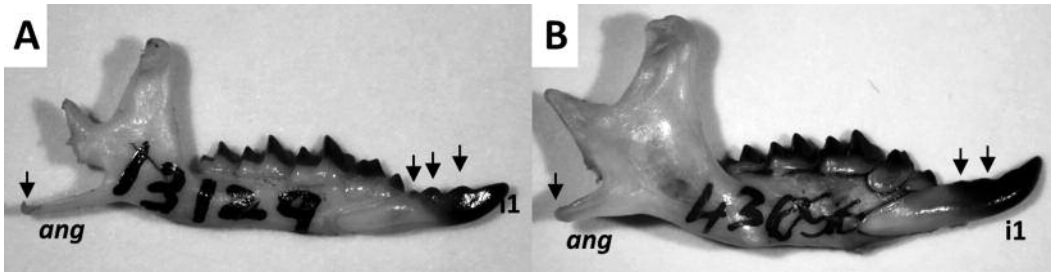

FIGURE 28. (*labial view*) Occlusal cusps on the incisor and the angular process (*ang*) of *Sorex hoyi* (A) and *Blarina brevicauda* (B).

36a. Mental foramen located beneath the m1 paraconid; the space between both cusps on the molars is relatively large (Figure 29A) . . . . . *Sorex dispar*
36b. Mental foramen located beneath the m1 protoconid or posteriorely; the space between both cusps on the molars is relatively small (Figure 29B) 37

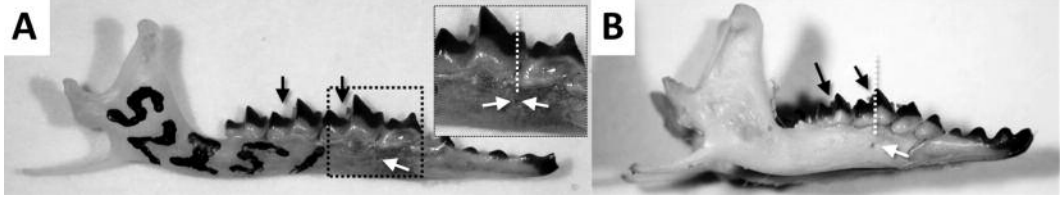

FIGURE 29. (*labial view*) Space between the cusps of molars (black arrows) and the relative position of the mental foramen (white arrows) in relation to the m1 paraconid and protoconid in *Sorex dispar* (A) and *S. maritimensis* (B).

37a. Postmandibular foramen present (Figure 30A); deep interdenticular spaces on i1 (Figure 30B) . . . 38
37b. Postmandibular foramen absent; shallow interdenticular spaces on i1 (Figure 30C) 39

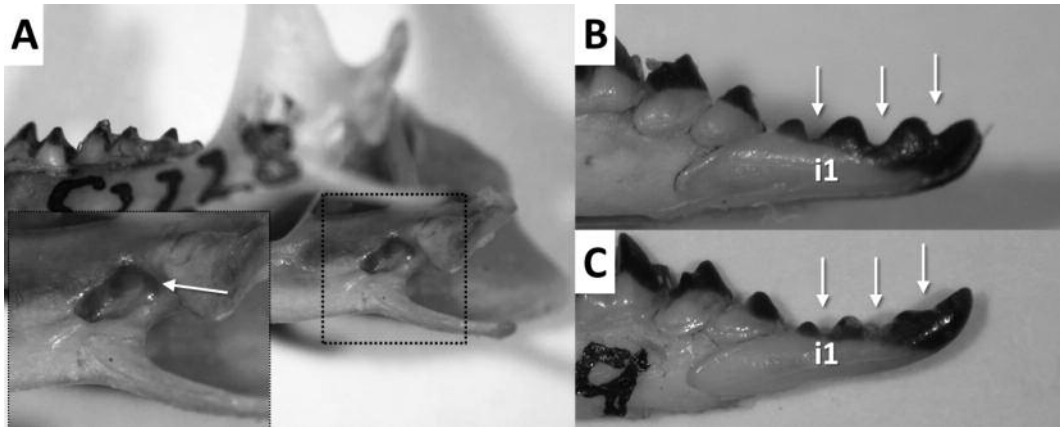

FIGURE 30. (*A. lingual view*; *B. and C. labial view*) Postmandibular foramen of *Sorex arcticus* (A) (arrow) as well as the interdenticular spaces (arrows) of the incisor of *S. arcticus* (B) and *S. palustris* (C).

38a. Height of coronoid process <4.5 mm (Figure 24) . . . . . *Sorex maritimensis*
38b. Height of coronoid process >4.5 mm (Figure 24) . . . . . *Sorex arcticus*

39a. Height of coronoid process >4.5 mm (Figure 24) . . . . . *Sorex palustris*
39b. Height of coronoid process <4.5 mm (Figure 24) 40

40a. Height of coronoid process <3.75 mm (Figure 24) . . . . . *Sorex cinereus*
40b. Height of coronoid process >3.75 mm (Figure 24) . . . . . *Sorex fumeus*

E. Carnivora (Canidae, Mephitidae, and Mustelidae)

41a. Two molars; very small to no diastema between c1 and p1; anterior part of the ramus under the canine thick (Figure 31A) 42

41b. Three molars; diastema between c1 and p1 about equal in size to p1 or larger; anterior part of the ramus under the canine slender (Figure 31B) 48

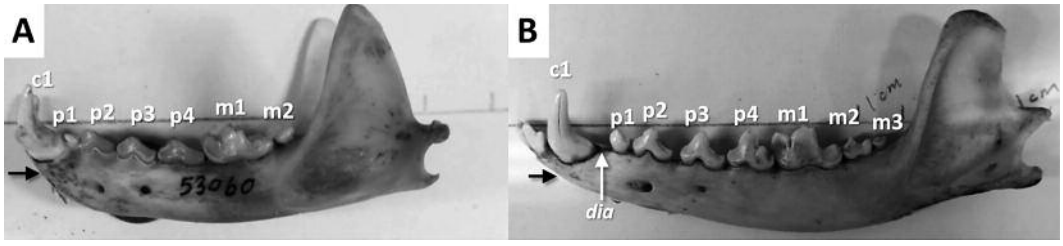

FIGURE 31. (*labial view*) Dental formula of mustelids (*Martes americana*) (A) and canids (*Vulpes lagopus*) (B) as well as the diastema (*dia*) present between c1 and p1 in canids. The black arrow shows the different shapes of the ramus below the canine in both species.

42a. Four premolars (Figure 31A) 43

42b. Three premolars (Figure 32) 44

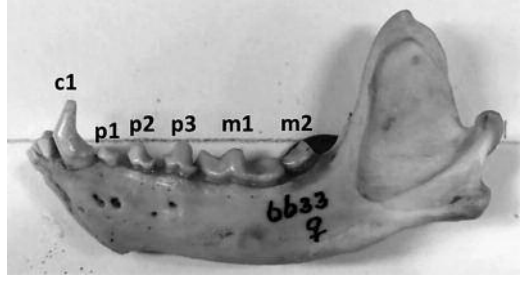

FIGURE 32. (*labial view*) The dentary bone of *Mustela*, *Neovison*, and *Mephitis mephitis* (shown in the figure), all composed of three premolars.

43a. Length of the mandibular tooth row <38 mm; posterior mental foramen located beneath the hypoconid of p3; coronoid process relatively sharp (Figure 33A) . . . . . *Martes americana*

43b. Length of the mandibular tooth row >38 mm; posterior mental foramen often located beneath the protoconid of p3; coronoid process rounded (Figure 33B) . . . . . *Martes pennanti*

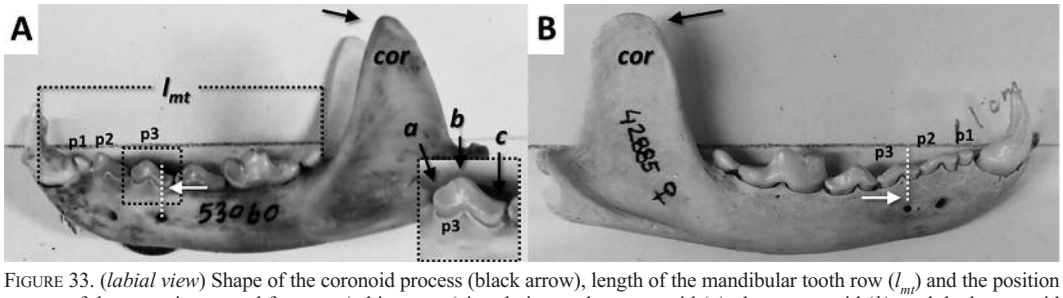

FIGURE 33. (*labial view*) Shape of the coronoid process (black arrow), length of the mandibular tooth row (l_{mt}) and the position of the posterior mental foramen (white arrow) in relation to the paraconid (*a*), the protoconid (*b*), and the hypoconid (*c*) of p3 in *Martes americana* (A) and *M. pennanti* (B).

44a. Bump present on the anterior part of the horizontal ramus approximately beneath p1 (Figure 34A); p1 clearly smaller than m2 (Figure 34C) . . . . . *Mephitis mephitis*

44b. Absence of a bump on the anterior part of the horizontal ramus (Figure 34B); p1 larger than m2 or about similar in size (Figure 34D) 45

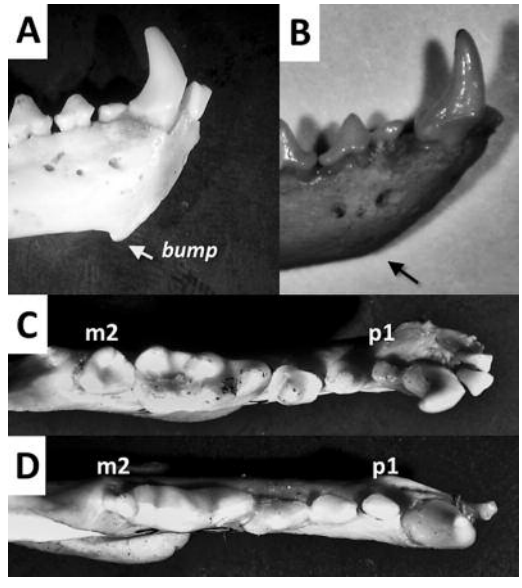

FIGURE 34. (*A. and B. labial view; C. and D. occlusal view*) Lower edge of the ramus of *Mephitis mephitis* (A) and *Mustela erminea* (B) and the size of m2 compared to p1 in *Mephitis mephitis* (C) and *Mustela erminea* (D).

45a. p2 often with a well-developed paraconid (Figure 35A); posterior edge of the vertical ramus with a distinct convex notch between the coronoid process and the condylar process (Figure 36A) . . . . . *Neovison vison*

45b. p2 often without a small anterior cusp (Figure 35B); posterior edge of the vertical ramus straight between the coronoid process and the condylar process (Figure 36B) 46

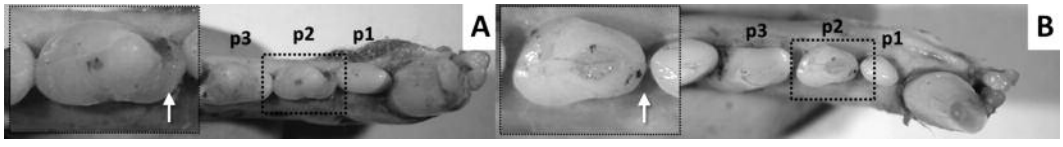

FIGURE 35. (*occlusal view*; *left: posterior*; *top: lingual*) The p2 of *Neovison vison* (A) and *Mustela frenata* (B).

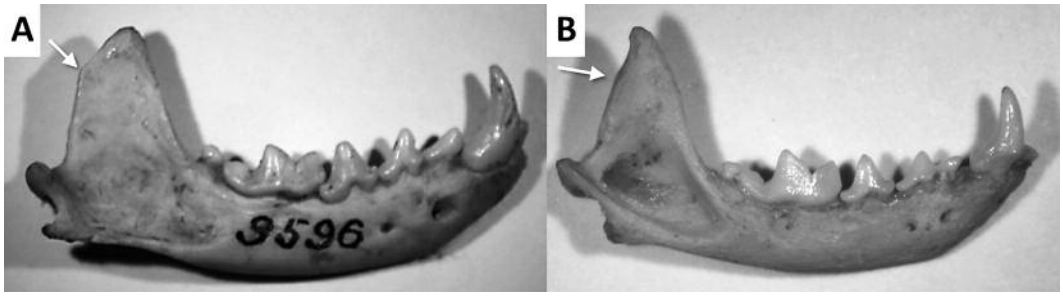

FIGURE 36. (*labial view*) Posterior edge of the vertical ramus (arrow) of *Neovison vison* (A) and *Mustela erminea* (B).

46a. Height of coronoid process <7.1 mm; length of mandibular tooth row <10 mm (Figure 37) . . . . . *Mustela nivalis*

46b. Height of coronoid process >7.1 mm; length of mandibular tooth row >10 mm (Figure 37) 47

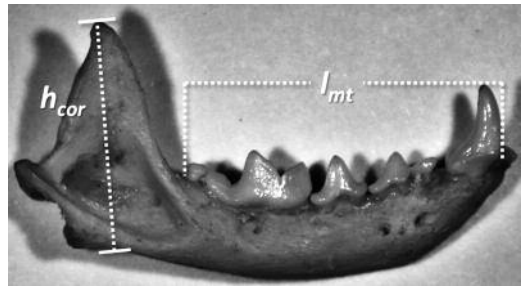

FIGURE 37. (*labial view*) Height of the coronoid process (h_{cor}) and length of the mandibular tooth row (l_{mt}) measured on *Mustela erminea*.

47a. Height of the coronoid process generally <10.5 mm; length of mandibular tooth row never >16 mm (Figure 37); posterior edge of the vertical ramus between the coronoid process and the condylar process relatively flat (Figure 38A) . . . . . *Mustela erminea*
47b. Height of the coronoid process generally >10.5 mm; length of mandibular tooth row often >16 mm (Figure 37); posterior edge of the vertical ramus between the coronoid process and the condylar process with a convex curve (Figure 38B) . . . . . *Mustela frenata*

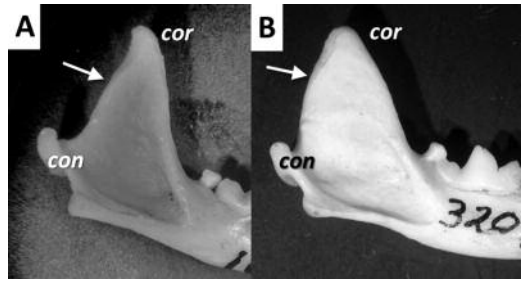

FIGURE 38. (*labial view*) Posterior edge of the vertical ramus (arrow) of *Mustela erminea* (A) and *M. frenata* (B).

48a. Presence of a clearly defined step on the lower edge of the horizontal ramus anterior to the angular process; diastemata between c1 and p1, between p1 and p2, and between p2 and p3 (Figure 39A) . . . . . *Urocyon cinereoargenteus*
48b. Lower edge of the horizontal ramus anterior to the angular process smooth, without a step; only one diastema between c1 and p1 (Figure 39B) 49

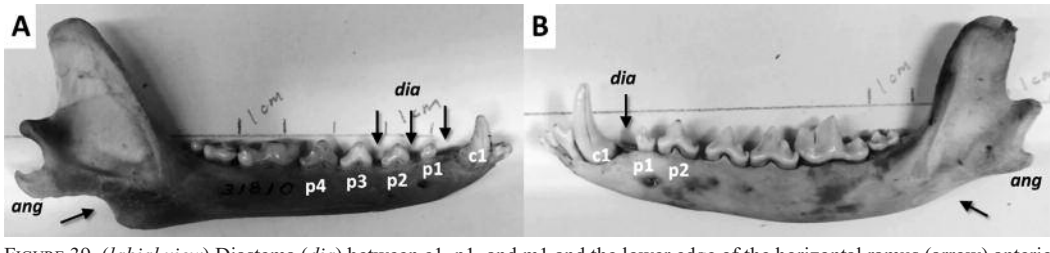

FIGURE 39. (*labial view*) Diastema (*dia*) between c1, p1, and m1 and the lower edge of the horizontal ramus (arrow) anterior to the angular process (*ang*) of *Urocyon cinereoargenteus* (A) and *Vulpes vulpes* (B).

49a. Anteroposterior length of the diastema between c1 and p1 smaller than p1 (Figure 40A) . . . *Vulpes lagopus*
49b. Anteroposterior length of the diastema between c1 and p1 about equal to p1 or larger (Figure 40B) . . . . . *Vulpes vulpes*

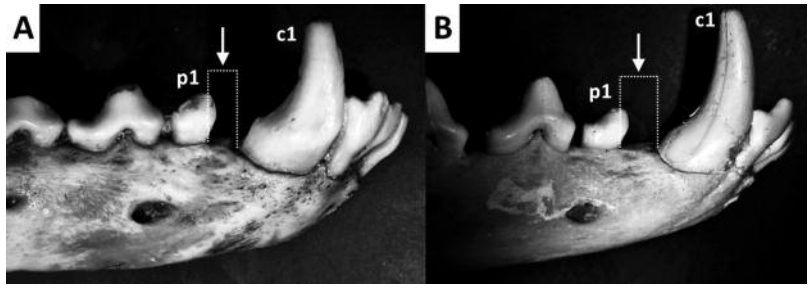

FIGURE 40. (*labial view*) Anteroposterior length of the diastema between c1 and p1 in relation to the anteroposterior length of p1 in *Vulpes lagopus* (A) and *V. vulpes* (B).

F. Chiroptera (Vespertilionidae)

50a. Three premolars (Figure 41A) 51
50b. Two premolars (Figure 41B) 54

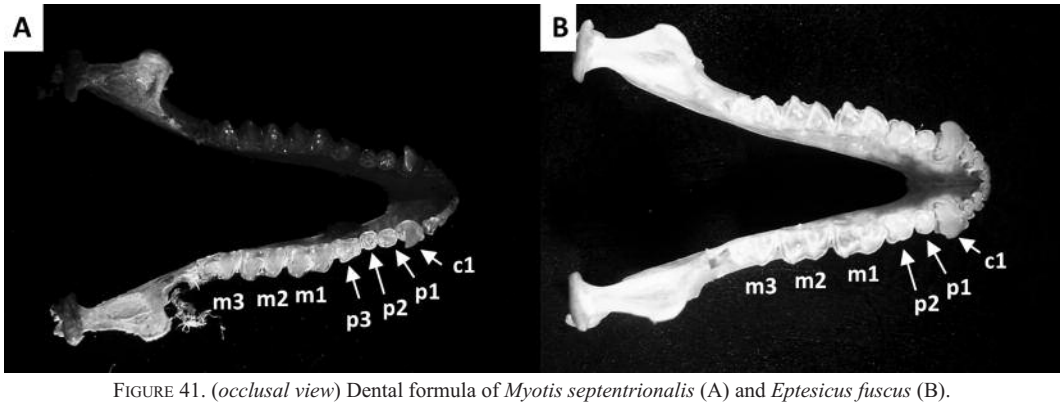

FIGURE 41. (*occlusal view*) Dental formula of *Myotis septentrionalis* (A) and *Eptesicus fuscus* (B).

51a. Mandibular length >11.5 mm (Figure 42); hypoconid of p3 with lingual crest directed medially creating a distinct lingual bulge (Figure 43A) . . . . . *Lasionycteris noctivagans*
51b. Mandibular length <11.5 mm (Figure 42); hypoconid of p3 without a distinct lingual bulge (Figure 43B) 52

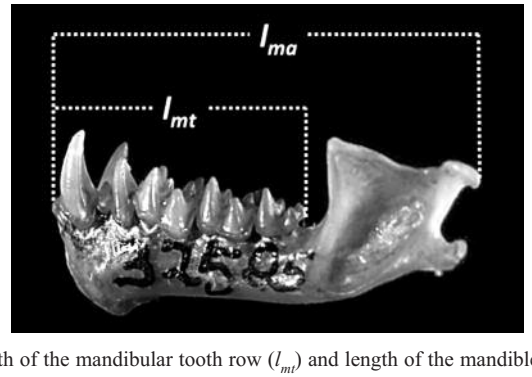

FIGURE 42. (*labial view*) Length of the mandibular tooth row (l_{mt}) and length of the mandible (l_{ma}) measured on Chiroptera (*Lasiurus cinereus*).

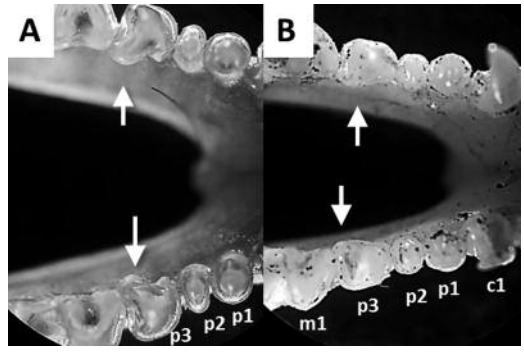

FIGURE 43. (*occlusal view*; *left: posterior*) Lingual crest of the p3 main cusp of *Lasionycteris noctivagans* (A) and *Myotis septentrionalis* (B).

52a. p3 rectangular, anteroposterior length greater than labiolingual width (Figure 44A); mandibular length generally ≥11mm (Figure 42) . . . . . *Myotis septentrionalis*
52b. p3 squared, anteroposterior length approximately equal to labiolingual width (Figure 44B); mandibular length <11mm (Figure 42) 53

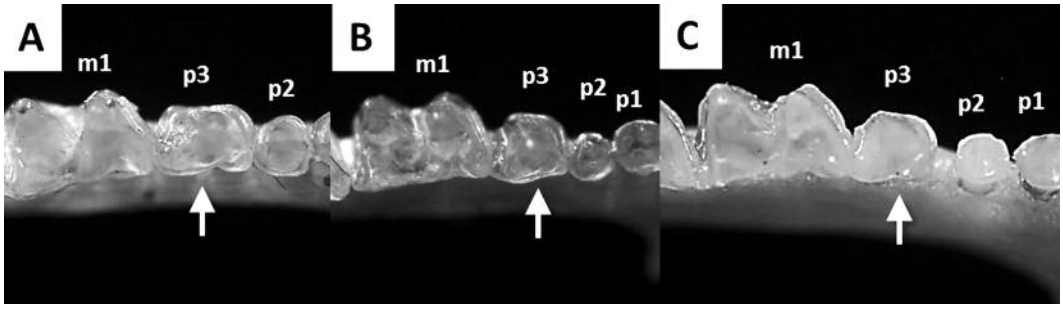

FIGURE 44. (*occlusal view*; *left: posterior*; *top: labial*) Shape of p3 in *Myotis septentrionalis* (A), *M. lucifugus* (B), and *M. leibii* (C).

53a. Mandibular length generally >10 mm; length of the mandibular tooth row generally >5.5 mm (Figure 42) . . . . . *Myotis lucifugus*
53b. Mandibular length generally <10 mm; length of the mandibular tooth row generally <5.5 mm (Figure 42) . . . . . *Myotis leibii*

54a. Mandibular length >12.5 mm (Figure 42) 55
54b. Mandibular length <12.5 mm (Figure 42) 56

55a. Mandibular length >14 mm (Figure 42); rounded coronoid process much taller than c1 (Figure 45A); p2 squared, with labiolingual width approximately equal to anteroposterior length (Figure 46A) . . . . . *Eptesicus fuscus*
55b. Mandibular length ≤14 mm (Figure 42); sharp coronoid process approximately same height as c1 (Figure 45B); p2 rectangular with labiolingual width greater than anteroposterior length (Figure 46B) . . . . . *Lasiurus cinereus*

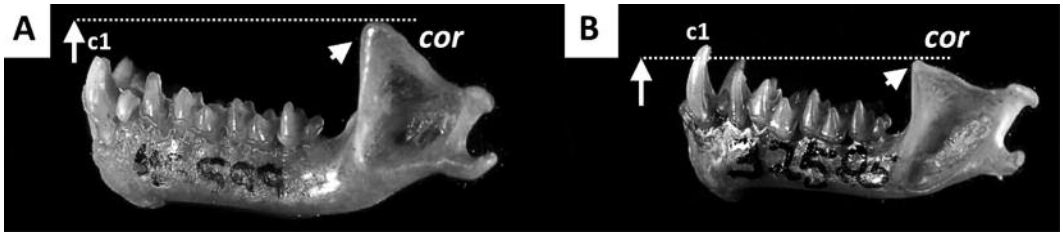

FIGURE 45. (*labial view*) Shape and height of the coronoid process (*cor*) of *Eptesicus fuscus* (A) and *Lasiurus cinereus* (B).

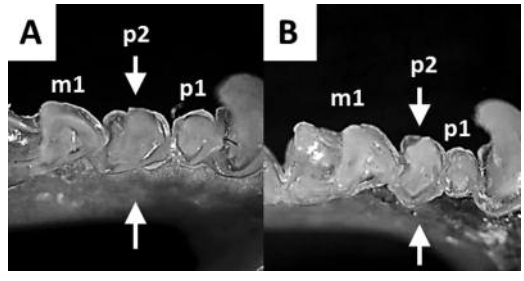

FIGURE 46. (*occlusal view*; *left: posterior*; *top: labial*) Shape of p2 of *Eptesicus fuscus* (A) and *Lasiurus cinereus* (B).

56a. Length of the mandibular tooth row <5 mm (Figure 42); small diastemata separate i2 from i3, i3 from c1, and p1 from p2; c1 approximately same height as p2 (Figure 47A) . . . . . *Perimyotis subflavus*
56b. Length of the mandibular tooth row >5 mm (Figure 42); no diastema between i2 and i3, i3 and c1, or p1 and p2; c1 taller than p2 (Figure 47B) . . . . . *Lasiurus borealis*

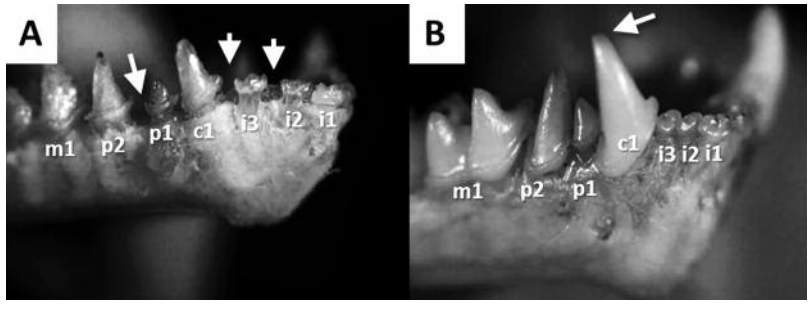

FIGURE 47. (*anterior view*) Relative size of c1 compared to p2 in *Perimyotis subflavus* (A) and *Lasiurus borealis* (B) as well as the diastemata between the incisors of *P. subflavus*.